NJC

Cite this: *New J. Chem.*, 2011, **35**, 2427–2434

www.rsc.org/njc

PAPER

New five-coordinate Ru(II) phosphoramidite complexes and their catalytic activity in propargylic amination reactions†

Andria K. Widaman,[a] Nigam P. Rath[ab] and Eike B. Bauer*[a]

Received (in Gainesville, FL, USA) 14th June 2011, Accepted 27th June 2011
DOI: 10.1039/c1nj20520j

The first five-coordinate, square-pyramidal ruthenium complexes of the general formula $[RuCl_2(PPh_3)_2L]$ have been prepared, where L is a phosphoramidite ligand. The new complexes were employed as catalysts for the amination reactions of propargylic esters (18 h, at room temperature or 45 °C, Cs_2CO_3) to give propargylic amines in isolated yields up to 94%.

Introduction

Propargylic alcohols (**1a** in Scheme 1) are important starting materials in organic synthesis.[1] They are readily available by addition of acetylides to ketones and can easily be functionalized further, *e.g.* by Sonogashira coupling[2] or by 1,3-dipolar cycloadditions to a triple bond.[3] The related propargylic amines (**2**) are important structural motifs found in natural products,[4] and are building blocks for bioorganic chemistry,[3] pharmaceutical production[5] and material science.[6] Due to the availability of propargylic alcohols **1a**, their conversion to propargylic amines is an attractive synthetic goal. Allylic substitution reactions are well established in organic synthesis;[7] however, their sister reaction—propargylic substitution—is far less investigated and understood.[8] Potential rearrangements of propargylic alcohols or their derivatives to allenes[9] or aldehydes[10] can lead to lower yields of the corresponding substitution reactions. Consequently, access to propargylic amines is mainly performed by other methods, such as the addition of alkynes to imines.[11]

The direct substitution of the –OH functionality in **1a** is challenging,[12] albeit some progress has been made in recent years.[13,14] Conversion of the poor –OH leaving group to a better one is a commonly employed strategy to facilitate such substitution reactions. Propargylic esters (**1b** in Scheme 1) are readily accessible and are therefore attractive for this purpose.[15] Early reports of the achiral amination of propargylic esters appeared in the literature in 1994, employing catalytic CuI and two equivalents of the amine.[16] Since then, other copper-catalyzed propargylic amination reactions of the corresponding esters have been published.[17] Furthermore, catalysis by other transition metals such as Rh[18a] and Ir,[18b] as well as that by Brønsted[19] and Lewis acids[20] has been employed. However, only one ruthenium catalyzed achiral propargylic amination reaction employing 1-arylprop-2-yn-1-ols has been reported.[21] To the best of our knowledge, ruthenium catalyzed amination reactions of propargylic acetates **1b** are thus far unknown. Some of the current catalytic systems for amination reactions of propargylic esters are restricted to internal propargylic acetates,[22] and, with a few exceptions,[8,18b,22] the catalytically active complexes are formed *in situ*. Consequently, their exact nature is unknown, making mechanistic investigations and rational ligand design more difficult.

As part of our long-standing interest in the catalytic activation of propargylic alcohols,[23] we are currently investigating ruthenium phosphoramidite complexes to serve that purpose. As open coordination sites are crucial for catalytic activity, we were interested in determining whether five-coordinate, square pyramidal ruthenium phosphoramidite complexes would exhibit activity in the title reaction. The commercial ruthenium complex $[RuCl_2(PPh_3)_3]$ (**5**) was a promising candidate for

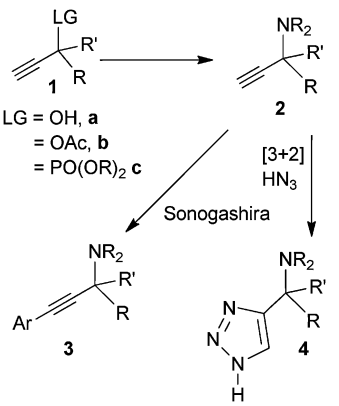

Scheme 1 Propargylic alcohols and their functionalization.

[a] *University of Missouri-St. Louis, Department of Chemistry and Biochemistry, One University Boulevard, St. Louis, MO 63121, USA. E-mail: bauere@umsl.edu; Fax: +1-314-516-5342; Tel: +1-314-516- 5311*
[b] *Center for Nanoscience, University of Missouri-St. Louis, St. Louis, MO 63121, USA*

† Electronic supplementary information (ESI) available: Experimental details, ^1H and ^{31}P NMR spectra of the ruthenium complexes, analytical data and ^1H and ^{13}C spectra of the catalysis products in Table 3. CCDC reference number 805144. For ESI and crystallographic data in CIF or other electronic format see DOI: 10.1039/c1nj20520j

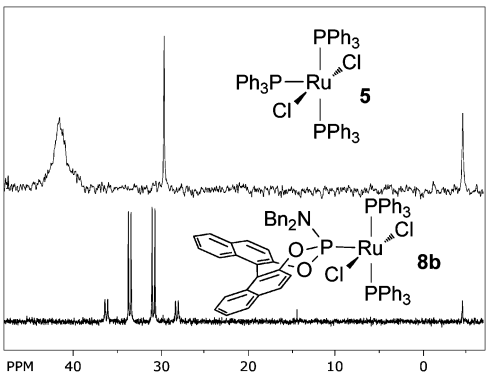

Fig. 1 ^{31}P NMR spectra of commercial $[RuCl_2(PPh_3)_3]$ (**5**, top) and $[RuCl_2(PPh_3)_2(\mathbf{7b})]$ (**8b**, bottom, partial spectrum), both in $CDCl_3$.

investigation as it displays such a coordination geometry, as shown by X-ray studies,[24] and is known for its rich chemistry with propargylic alcohols.[25] Partially due to its coordinative unsaturation, complex **5** exhibits dynamic behavior in solution;[26] for example, it can form chloro-bridged dimers, such as **6** in eqn (1), or oligomers. These bridge systems can be very stable[27] and have been described as exhibiting decreased catalytic activity for some organic transformations.[28]

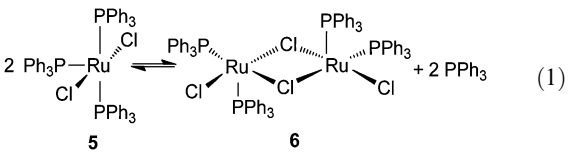

(1)

The dynamic behavior of complex **5** can be best observed in the ^{31}P NMR spectrum, which exhibits only a broad peak around 42 ppm, as confirmed by measurements in our laboratory (Fig. 1, top).

We speculated that complex **5** could be modified to give a more stable, monomeric, five-coordinate architecture in solution. Such a stabilized complex could exhibit more predictable catalytic activity compared to multiple species resulting from the dynamic solution behavior of $[RuCl_2(PPh_3)_3]$. Herein, we report the synthesis of complexes of the general formulation $[RuCl_2(PPh_3)_2L]$ (L = phosphoramidite ligand) and their catalytic application in propargylic amination reactions.

Results and discussion

Synthesis and characterization of the ruthenium complexes

Accordingly, we first sought access to appropriate ruthenium phosphoramidite[29] complexes. When the known[29c] phosphoramidite ligand (R)-**7a** was added to a solution of complex **5**, an immediate color change to blue took place (Scheme 2). After 20 min, removing the solvent and washing the residue with several portions of cold Et_2O afforded the complex $[RuCl_2(PPh_3)_2((R)\text{-}\mathbf{7a})]$ (**8a**) as a grey solid in 41% isolated yield. Similarly, the known[29c] phosphoramidite ligand (R)-**7b** could be converted to the green complex $[RuCl_2(PPh_3)_2((R)\text{-}\mathbf{7b})]$ (**8b**) in 80% isolated yield.

The new complexes were fully characterized by multinuclear NMR, MS and elemental analysis, which confirmed the general formulation $[RuCl_2(PPh_3)_2((R)\text{-}\mathbf{7})]$ (spectra are provided in the

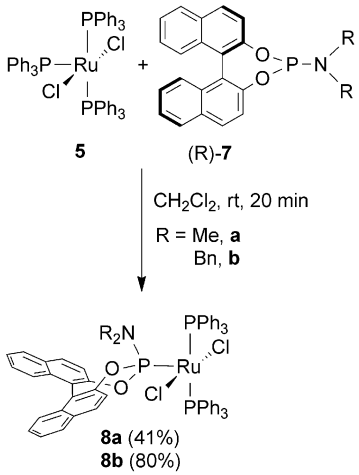

Scheme 2 Synthesis of ruthenium phosphoramidite complexes **8**.

Supplementary Information†). The FAB mass spectra showed a molecular ion peak for both complexes. In addition, a diagnostic fragmentation pattern was present due to loss of Cl, PPh_3 and (R)-**7** ligands. The ^1H NMR spectra exhibited a complex aromatic region, but the NCH_3 and NCH_2 units gave resonances in the aliphatic region at 1.9 and 4.2 ppm, respectively. Due to the numerous aromatic carbon atoms, a complex aromatic region in the ^{13}C NMR spectra resulted, but again, the NCH_3 and NCH_2 groups gave distinct signals at 37.8 and 48.9 ppm.

The most striking feature of the new complexes were their sharp ^{31}P NMR peaks, as exemplified by complex **8b**, whose partial ^{31}P NMR spectrum is shown in Fig. 1 (bottom). The two PPh_3 ligands exhibited a well-resolved AB pattern at 34.6 and 29.9 ppm, coupled to the phosphoramidite ligand (R)-**7b** (38.8 Hz). Due to coupling to the two PPh_3 ligands, the phosphoramidite ligand appeared as a triplet at 171.3 ppm (the full spectrum is provided in the Supplementary Information). As opposed to the starting material **5**, the spectra of complexes **8** are well resolved and show no sign of dynamic behavior in solution. Thus, replacement of one PPh_3 ligand in **5** by the ligands **7** resulted in a configurationally more stable structure.

To unequivocally establish the structure of the new complexes, an X-ray diffraction analysis was performed for complex **8b** (Fig. 2), confirming its slightly distorted, five-coordinate, square-pyramidal geometry, similar to that of **5**.[24] Key bond lengths and angles are compiled in Table 1 and, for comparison, the corresponding values for the structurally related complex $[RuCl_2(PPh_3)_3]$ (**5**) are also listed.[24]

In the complex **8b**, specifically the apical PPh_3 ligand in the position *trans* to the open coordination site is exchanged by the phosphoramidite (R)-**7b**. The two PPh_3 ligands occupy approximately *trans* positions, with an angle of 164.08(3)°. The two chloro ligands are also located approximately *trans* to each other, as seen by their Cl(1)–Ru–Cl(2) angle of 155.20(3)°. The phosphoramidite ligand and the two PPh_3 ligands form angles of 95.73(3) and 99.67(3)°, respectively.

The Ru–P bond lengths are significantly shorter for the phosphoramidite ligand **7b** (2.1561(9) Å) than for the PPh_3 ligands (2.3793(9) and 2.4072(9) Å). We have previously

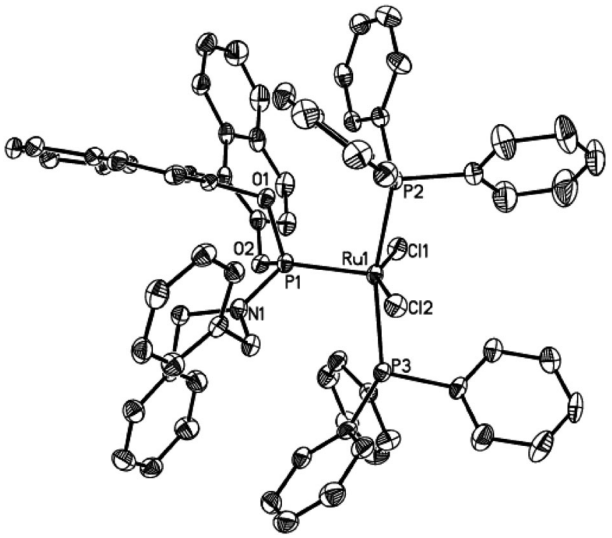

Fig. 2 Molecular structure of **8b** (depicted with 50% probability ellipsoids; H atoms are omitted for clarity). Key bond lengths and bond angles are listed in Table 1.

Table 1 Key bond lenght (Å) and angles (°)

	8b	$[RuCl_2(PPh_3)_3]$[24]
Ru(1)–Cl(1)	2.3779(8)	2.387(7)
Ru(1)–Cl(2)	2.3700(8)	2.388(7)
Ru(1)–P(1)	2.1561(9)	2.230(8)
Ru(1)–P(2)	2.3793(9)	2.374(6)
Ru(1)–P(3)	2.4072(9)	2.412(6)
P(1)–N(1)	1.657(3)	—
P(1)–Ru(1)–Cl(1)	95.50(3)	92.9 (2)
P(1)–Ru(1)–Cl(2)	109.28(3)	109.9 (2)
Cl(1)–Ru(1)–Cl(2)	155.20(3)	157.2 (2)
P(1)–Ru(1)–P(2)	95.73(3)	101.1(2)
Cl(2)–Ru(1)–P(2)	85.66(3)	82.1(2)
Cl(1)–Ru(1)–P(2)	91.19(3)	93.4(2)
P(1)–Ru(1)–P(3)	99.67(3)	101.4 (2)
Cl(2)–Ru(1)–P(3)	85.49(3)	83.7(2)
Cl(1)–Ru(1)–P(3)	91.31(3)	92.4 (2)
P(2)–Ru(1)–P(3)	164.08(3)	156.4(2)

observed this difference in bond length[30] and tentatively attributed the shortened bond to the increased π-acidity of the phosphoramidite ligands **7** compared to PPh_3. It has been previously described in the literature, that phosphine ligands PX_3 with electronegative X substituents, such as F, promote π-backbonding, resulting in shortened M–P bond lengths.[31] Accordingly, increased π-acidity has been ascribed to phosphoramidites.[29a] In addition, the coordination site *trans* to the phosphoramidite ligand is unoccupied, thus no competition between ligands for the d-electrons of the metal takes place. Both effects result in a higher degree of metal-to-ligand back-bonding, which would shorten the Ru–P bond.

In addition, σ-effects may contribute to a shortening of this bond. Compounds PX_3 with electronegative substituents X increase the σ-character of the lone pair on the phosphorus.[32] Furthermore, σ-bonds in position *trans* to a ligand weaken the ligand bond to the metal center, but the phosphoramidite ligand in complex **8b** lacks a ligand in that position. These two σ-effects might also contribute to a shorter Ru–P bond of the phosphoramidite ligand. The combination of both the σ- and π-influence results in a shorter Ru–P bond length for the phosphoramidite ligand in complex **8b** (2.1561(9) Å), which is even shorter than the corresponding apical Ru–PPh_3 bond in the "parent" complex $[RuCl_2(PPh_3)_3]$ (2.230(8) Å).

To better understand the increased stability of complexes **8** in solution, the structural parameters of complex **8b** are compared to those of complex $[RuCl_2(PPh_3)_3]$ (Table 1). The P(2)–Ru(1)–P(3) angle for complex **8b** (164.08(3)°) is larger than the corresponding angle in the complex $[RuCl_2(PPh_3)_3]$ (156.4(2)°). In turn, the P(1)–Ru(1)–P(2) and P(1)–Ru(1)–P(3) angles in **8b** (95.73(3)° and 99.67(3)°) are smaller than the corresponding angles in $[RuCl_2(PPh_3)_3]$ (101.1(2)° and 101.4 (2)°). These values suggest diminished steric bulk of the phosphoramidite ligand in **8b** compared to PPh_3 in the complex $[RuCl_2(PPh_3)_3]$. Albeit the phosphoramidite ligand **7b** contains more atoms, it may have a smaller cone angle than PPh_3.[33] Consequently, the two remaining PPh_3 ligands in **8b** are not as strongly repelled by the phosphoramidite ligand as they are by the apical PPh_3 ligand in $[RuCl_2(PPh_3)_3]$. Due to the decreased steric demand of the phosphoramidite ligands in complexes **8**, it is possible that their tendency to undergo a dissociative dimerization process according to eqn (1) is diminished, resulting in an increased stability of the monomeric structures.

Catalysis

We subsequently employed the new complexes as catalysts in propargylic amination reactions. The higher yielding complex **8b** was employed for screening reactions and for all isolated yields, and complex **8a** showed comparable activity as shown by GC measurements. Initial screening reactions revealed that employment of propargylic alcohols gave at most moderate conversions to the corresponding propargylic amines.

However, when the corresponding propargylic acetates **9** were employed in the presence of a base, the conversions were higher (Table 2). The bases NEt_3 and NaOH gave only trace quantities of the expected products. Using the sterically hindered base diazabicycloundecene (DBU) resulted in higher conversions (entries 1 and 2), but a 90 °C temperature was required. In addition, as determined by GC-MS, DBU derivatives formed, complicating purification. This issue was resolved by using Cs_2CO_3 (Table 2, entries 3–9), which was superior in our screening experiments; however, we observed solvent-dependencies for that base. In THF or C_6H_5Cl, only low conversions were observed at 90 °C (entry 3), but 53% conversion and fewer side products were observed in THF at 22 °C (entry 4). In *i*-PrOH, up to 72% conversion was observed at 22 °C (entry 5) and was increased only slightly by employing heat (entries 6–8), but the isolated yields never exceeded 37% (entries 6 and 7). We speculate that the acetate starting material decomposes under the conditions in entries 6 to 8. However, employment of CH_2Cl_2 resulted not only in complete consumption of the acetate starting material at room temperature, but also in high yields of the corresponding propargyl amine (entry 9). The "parent" propargylic acetate $HC{\equiv}CCH_2OAc$ gave only minimal formation of the corresponding propargylic amine (entry 10). No product formation

Table 2 Screening reactions

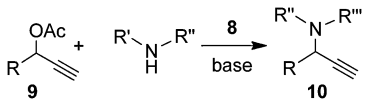

Entry[a]	R,R′,R′′	Base/solvent Temperature	Conversion[b] (isolated yield)
1	Ph, Bn, Me	DBU/C_6H_5Cl 90 °C	17%[c]
2	C_5H_{11}, Bn, Me	DBU/C_6H_5Cl 90 °C	50%[c] (30%)
3	C_5H_{11}, Bn, Me	$CsCO_3$/THF or C_6H_5Cl 90 °C	8–14%
4	Ph, Bn, Me	$CsCO_3$/THF 22 °C	53%
5	Ph, Bn, Me	$CsCO_3$/*i*-PrOH 22 °C	72%
6	Ph, Bn, Me	$CsCO_3$/*i*-PrOH 90 °C	100%[d] (37%)
7	C_5H_{11}, Bn, Me	$CsCO_3$/*i*-PrOH 90 °C	75% (36%)
8	C_5H_{11}, Bn, Bn	$CsCO_3$/*i*-PrOH 90 °C	75%
9[e]	Ph, Bn, Me	$CsCO_3$/CH_2Cl_2 22 °C	100% (76%)
10[e]	H, Bn, Me	$CsCO_3$/CH_2Cl_2 22 °C	2%

[a] Acetate (0.23 mmol), amine (0.46 mmol), base (0.8 mmol), catalyst **8b** (0.01 mmol) in the solvent (1 mL) in a screw-capped vial for one day. [b] Determined by GC relative to the acetate starting material. Isolated yields after column chromatography. [c] DBU produced a complex reaction mixture, in which DBU derivatives were identified. [d] No acetate starting material was detected but the isolated yields never exceeded 37%, presumably due to substrate decomposition during the reaction. [e] Acetate (0.2 mmol), amine (0.8 mmol), base (0.4 mmol), catalyst **8b** (0.01 mmol) in the solvent (1 mL) in a screw-capped vial for one day.

was observed with primary amines or anilines, and no reaction took place without ruthenium catalysts **8**.

Under optimized conditions, we employed the title reaction for a variety of propargylic acetates **11** and amines **12** and the results are compiled in Table 3. Employing a molar ratio of 1 (propargyl acetate **11**): 3.5 to 4 (amine **12**) and shaking for 18 h at room temperature or 45 °C in CH_2Cl_2 afforded the propargylic amines **13** that were isolated by column chromatography or flash filtration in 55–94% yield. Two equivalents of Cs_2CO_3 were added to the reaction mixture to help drive the reaction to completion. As Table 3 demonstrates, the reaction shows a broad substrate scope. Both secondary (**11b**) and tertiary (**11a**,**c**,**d**) propargylic acetates were aminated with secondary amines, and both phenyl and alkyl substituents can be tolerated on the propargylic ester. The tertiary acetates required slightly elevated temperatures for the reaction to go to completion. The substituents on the amine exhibited different levels of steric congestion; benzyl, methyl, isopropyl and cyclohexyl amines all were successfully employed in the reaction with only slight differences in the isolated yields. The chiral amine (R)-(**14**) also was converted to the corresponding propargylamine **15** (entry 10); during the reaction, a stereocenter at the triple bond is formed, and the amine **15** was isolated as a 1 : 1 mixture of diastereomers, as assessed by ^{1}H NMR spectroscopy.

Table 3 Propargylic amination reactions

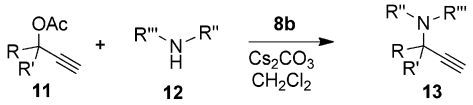

Entry[a]	Substrates	Temperature	Product	Isolated yield
1	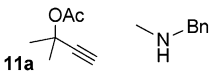	45 °C	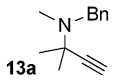	71%
2	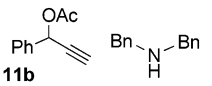	22 °C	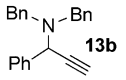	72%
3	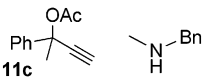	45 °C	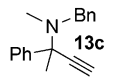	75%
4	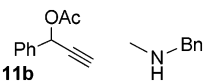	22 °C	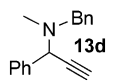	76%
5	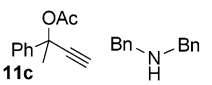	45 °C	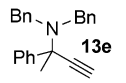	64%
6	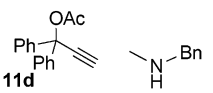	45 °C	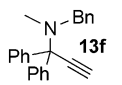	84%
7	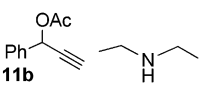	22 °C	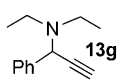	71%
8	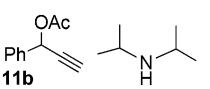	22 °C	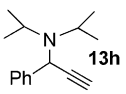	55%
9	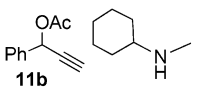	22 °C	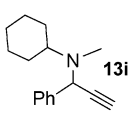	94%
10	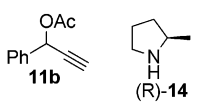	22 °C	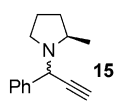	82%[b]

[a] Typical conditions: Substrate (0.32 mmol), amine (1.10 mmol), Cs_2CO_3 (0.64 mmol) and **8b** (5 mol%), 18 h in CH_2Cl_2 (0.5 mL) in a screw-capped vial at the temperature indicated in the table. The products were isolated by column chromatography or filtration utilizing silica or alumina. [b] The product was isolated as a 1 : 1 mixture of diastereomers (as assessed by ^{1}H NMR).

The substrate scope presented in Table 3 complements that of other catalytic systems employed for the title reaction. Copper-pyridine-2,6-bisoxazoline complexes were reported to be catalytically active in the amination of secondary propargylic acetates with primary amines,[17b] while copper-diphosphine complexes were reported to show catalytic activity for secondary propargylic acetates and secondary amines.[17c] The unsaturated complexes **8a** and **8b** are able to aminate secondary and tertiary propargylic acetates.

During synthesis of the propargylic amines, a new stereogenic center is formed. For most of the propargylic amines in Table 3, no literature precedent for the determination of enantiomeric excesses exists, and our attempts to chromatographically separate enantiomers by chiral GC or HPLC have failed thus far. However, the optical rotation of compound **13b** in Table 3 was measured to be zero. Furthermore, no diastereomeric excess for compound **15** was obtained, so the reactions in Table 3 presumably do not provide an enantiomeric excess. Ligand modifications to promote enantiodifferentiation for the title reaction are currently underway.

Mechanistically, the reaction might proceed either through a transition-metal-stabilized propargyl cation (**16**)[34] or an allenylidene intermediate (**17**, Scheme 3).[17b,c]

To determine the involvement of a potential allenylidene intermediate, we performed a stoichiometric reaction between complex **8b** and propargylic acetate **11b**, but no evidence for allenylidene formation was obtained. On the contrary, the internal propargylic acetate **18** cannot be aminated under the conditions in Table 3 to give the corresponding propargylamine **19** [eqn (2)], despite the structural diversity among propargylic acetates employed in Table 3. Internal propargylic alcohols or their derivatives cannot be easily converted to allenylidene complexes,[35] which suggests, indirectly, that an allenylidene intermediate **17** may be involved.

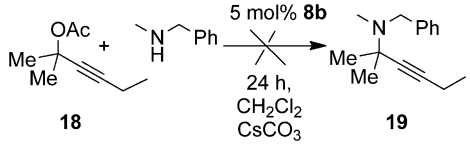

(2)

A potential allenylidene intermediate also could explain why the acetate of the parent propargylic alcohol showed only minimal product formation (Table 2, entry 10, with R = H for **9**). For this substrate, an intermediate allenylidene complex **17** would result, where R and R′ are H (Scheme 3). Such allenylidene complexes are unknown,[35] and could not undergo the catalytic cycle as depicted in Scheme 3.

Furthermore, metal-stabilized carbocations are known for transition metals such as Mo[36a] or Co.[36b] To the best of our knowledge, ruthenium-stabilized carbocations have not been reported in the literature and have not been suggested as intermediates in propargylic substitution reactions,[34] which suggests that the title reaction proceeds through an allenylidene intermediate.

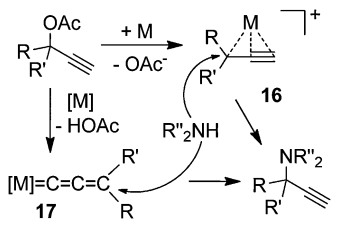

Scheme 3 Simplified mechanistic picture.

In any event, further experiments are necessary to firmly establish a mechanism for the reaction.

Conclusion

In conclusion, we have synthesized for the first time five-coordinate, square pyramidal ruthenium complexes of the general formula $[RuCl_2(PPh_3)_2L]$, where L is a phosphoramidite ligand, one example of which has been characterized structurally. As seen by sharp resonances in the NMR spectra, the new complexes exhibited no dynamic behavior in solution as opposed to their precursor, $[RuCl_2(PPh_3)_3]$. The new complexes were employed successfully in propargylic amination reactions of propargylic acetates (room temperature or 45 °C, 18 h, Cs_2CO_3 as auxiliary base) to give the corresponding propargylic amines in 55 to 94% isolated yields. It is the first ruthenium—based catalytic system for the amination of propargylic acetates, and thus, we introduce the complexes $[RuCl_2(PPh_3)_2L]$ as a new, tunable platform to promote the title reaction under mild conditions. Mechanistic investigations and further experiments to widen the substrate scope are currently underway.

Experimental section

General

Chemicals were treated as follows: diethyl ether, distilled from Na/benzophenone; CH_2Cl_2, distilled from $CaCl_2$; petroleum ether and ethyl acetate used as received. $[RuCl_2(PPh_3)_3]$ (**5**, Strem), amine substrates for catalytic experiments, Cs_2CO_3, silica (all Aldrich), and other materials used as received. "(R)-BINOL-*N*,*N*-dimethyl-phosphoramidite" (R)-**7a**,[29c] "(R)-BINOL-*N*,*N*-dibenzyl-phosphoramidite" (R)-**7b**,[29c] and the propargylic acetates **11a**,[37a] **11b**,[17b] **11c**,[37b] and **11d**[37c] were synthesized with slight modification to literature procedures. All reactions were carried out under nitrogen employing standard Schlenk techniques; workups and catalytic experiments were carried out in open air.

NMR spectra were obtained at room temperature on a Bruker Avance 300 MHz or a Varian Unity Plus 300 MHz instrument and referenced to a residual solvent signal; all assignments are tentative. GC/MS spectra were recorded on a Hewlett Packard GC/MS System Model 5988A. Exact masses were obtained on a JEOL MStation [JMS-700] Mass Spectrometer. IR spectra were recorded on a Thermo Nicolet 360 FT-IR spectrometer. Elemental analyses were performed by Atlantic Microlab Inc., Norcross, GA, USA.

[($RuCl_2(PPh_3)_2$((R)-BINOL-*N*,*N*-dimethyl-phosphoramidite)] (8a). To a Schlenk flask containing phosphoramidite (R)-**7a** (83 mg, 0.23 mmol) and $[RuCl_2(PPh_3)_3]$ (**5**, 215 mg, 0.22 mmol), CH_2Cl_2 (4 mL) was added and the solids dissolved. The dark blue solution was stirred at room temperature for 20 min. The solvent was then removed under vacuum, giving

dark blue solids. The solids were washed with diethyl ether (3 × 2 mL) to obtain **8a** as a light blue solid (0.097 g, 0.09 mmol, 41%). Found: C, 66.0; H, 4.7. $C_{58}H_{48}Cl_2NO_2P_3Ru$ requires C, 66.0; H, 4.6%.[38] ^{1}H-NMR δ_H (300.13 MHz; $CDCl_3$; Me_4Si) 7.56–7.91 (m, 12H, arom), 7.10–7.45 (m, 23H, arom), 6.98–7.06 (m, 5H, arom), 6.77–6.82 (m, 2H, arom), 1.91 (s, 3H, CH_3), 1.88 (s, 3H, CH_3); ^{13}C-NMR δ_C (75.5 MHz; $CDCl_3$; Me_4Si; partial)[39] 37.8 (2CH_3); ^{31}P{^{1}H}-NMR δ_P ($CDCl_3$; H_3PO_4) 173.5 (t, $^2J_{PP}$ = 40.7 Hz, phosphoramidite), 41.0, 34.7 (ABq, $^2J_{AB}$ = 332.6 Hz, $^2J_{PP}$ = 38.8 Hz, 2PPh_3). HRMS calcd for $C_{58}H_{48}{}^{35}Cl_2NO_2P_3{}^{102}Ru$: 1055.1317. Found 1055.1345. MS (FAB, 4-NBA) *m*/*z*: 1055 (**8a**$^+$, 20%), 1020 ([**8a**–Cl]$^+$, 15), 793 ([**8a**–PPh_3]$^+$, 65), 696 ([$RuCl_2(PPh_3)$]$^+$, 30).

[($RuCl_2(PPh_3)_2$((R)-BINOL-*N*,*N*-dibenzyl-phosphoramidite)-(Et_2O)] (8b). To a Schlenk flask containing phosphoramidite (R)-**7b** (0.1248 g, 0.244 mmol) and [$RuCl_2(PPh_3)_3$] (**5**, 0.233 g, 0.243 mmol), CH_2Cl_2 (4 mL) was added and the solids dissolved. The green solution was stirred at room temperature for 20 min. The solvent was then removed under vacuum, giving dark green solids. The solids were washed with diethyl ether (3 × 2 mL) to obtain **8b** as a green solid (0.234 g, 0.194 mmol, 80%). Found: C, 69.2; H, 5.1. $C_{70}H_{56}Cl_2NO_2P_3Ru{\cdot}(Et_2O)$ requires C, 69.3; H, 5.2%.[38] ^{1}H-NMR δ_H (300.13 MHz; $CDCl_3$; Me_4Si) 7.95 (d, $^3J_{HH}$ = 8.0 Hz, 2H, arom), 7.85 (d, $^3J_{HH}$ = 9.0 Hz, 2H, arom), 7.63–7.72 (m, 9H, arom), 7.42–7.56 (m, 9H, arom), 7.03–7.36 (m, 26H, arom), 6.91–6.94 (d, $^3J_{HH}$ = 8.0 Hz, 4H, arom), 6.50 (br, 1H, CHH′Ph), 6.44 (d, $^3J_{HH}$ = 8.9 Hz, 1H, CHH′Ph), 4.21 (br, 2H, CH_2Ph); ^{13}C-NMR δ_C (75.5 MHz; $CDCl_3$; Me_4Si; partial)[39] 48.97 (NCH_2), 48.91 (NCH_2′); ^{31}P{^{1}H}-NMR δ_P ($CDCl_3$; H_3PO_4) 171.3 (t, $^2J_{PP}$ = 38.8 Hz, phosphoramidite), 34.6, 29.9 (ABq, $^2J_{AB}$ = 326.9 Hz, $^2J_{PP}$ = 38.8 Hz, 2PPh_3). HRMS calcd for $C_{70}H_{56}{}^{35}Cl_2NO_2P_3{}^{102}Ru$: 1207.1943. Found: 1207.1909. MS (FAB, 4-NBA) *m*/*z*: 1207 (**8b**$^+$, 4%), 1172 ([**8b**–Cl]$^+$, 2), 945 ([**8b**–PPh_3]$^+$, 24), 910 ([$RuCl(PPh_3)$((R)-**7b**)]$^+$, 15), 648 ([RuCl((R)-**7b**)]$^+$, 24).

Representative catalytic procedures (Table 3)

1-Methyl-1-phenyl-*N*,*N*-dibenzyl-2-propyn-1-amine (13e). To a screw-capped vial containing [$RuCl_2(PPh_3)_2$((R)-**7b**)] (**8b**, 0.013 g, 0.011 mmol) and Cs_2CO_3 (0.133 g, 0.41 mmol), CH_2Cl_2 (0.5 mL) was added to dissolve the metal complex, followed by 1-methyl-1-phenyl-2-propynyl acetate (**11c**, 0.039 g, 0.21 mmol) and dibenzylamine (0.167 g, 0.85 mmol) under open atmosphere. The mixture was heated in a heating block at 45 °C for 18 h. The residue was purified by flash chromatography (1 × 10 cm SiO_2, petroleum ether/EtOAc 10 : 1 v/v), then concentrated under reduced pressure to obtain **13e** as a yellow oil (0.043 g, 0.13 mmol; 64%). ^{1}H-NMR δ_H (300.13 MHz; $CDCl_3$; Me_4Si) 7.83–7.86 (m, 2H, Ph), 7.02–7.33 (m, 13H, Ph), 3.63 (s, 4H, 2CH_2), 2.66 (s, 1H, C≡CH), 1.30 (s, 3H, CH_3); ^{13}C{^{1}H}-NMR δ_C (75.5 MHz; $CDCl_3$; Me_4Si) 145.7 (Ph), 141.7 (Ph), 128.3 (Ph), 128.0 (Ph), 127.4 (Ph), 126.53 (Ph), 126.50 (Ph), 83.5 (*C*≡CH), 75.2 (C≡*C*H), 65.6 (Ph*C*), 55.7 (2CH_2), 33.4 (CH_3). HRMS calcd for $C_{24}H_{23}N$: 325.1830. Found: 325.1819. MS (EI) *m*/*z*: 325 (3%), 310 (22), 248 (8), 181 (7), 129 (56), 91 (100). IR (neat oil) ν_{max}/cm^{-1} 3294m (C≡C–H), 3061m, 3027m, 2924m, 2846m, 1493m, 1447m, 697s.

2-Methyl-*N*-(1-phenyl-2-propynyl)pyrrolidine (15). To a vial containing [$RuCl_2(PPh_3)_2$((R)-**7b**)] (**8b**, 0.014 g, 0.012 mmol) and Cs_2CO_3 (0.151 g, 0.46 mmol), CH_2Cl_2 (0.5 mL) was added to dissolve the metal complex, followed by 1-phenyl-2-propynyl acetate (**11b**, 0.040 g, 0.23 mmol) and 2-methylpyrrolidine (**14**, 0.077 g, 0.90 mmol) under open atmosphere. The mixture was shaken for 18 h at room temperature. The residue was purified by vacuum filtration through Al_2O_3 in a fritted funnel with petroleum ether and ethyl acetate (10 : 1), then concentrated under reduced pressure to give yellow oil **15** as a mixture of diastereomers (1 : 1, ^{1}H NMR) (0.037 g, 0.19 mmol; 82%). ^{1}H-NMR δ_H (300.13 MHz; $CDCl_3$; Me_4Si; the starred signals* denote the second diastereomer) 7.51 (d, $^3J_{HH}$ = 7.3 Hz, 2H, Ph), 7.46 (d, $^3J_{HH}$ = 6.7 Hz, 2H, Ph*), 7.17–7.30 (m, 6H, Ph/Ph*), 4.87 (d, $^4J_{HH}$ = 2.1 Hz, 1H, Ph-CH), 4.80 (d, $^4J_{HH}$ = 2.2 Hz, 1H, PhCH*), 3.04–3.10 (m, 1H, H_3CCH), 2.65–2.83 (m, 2H, NCH_2), 2.52–2.61 (m, 1H, H_3CCH*), 2.41 (d, $^4J_{HH}$ = 2.1 Hz, 1H, C≡CH), 2.40 (d, $^4J_{HH}$ = 2.2 Hz, 1H, C≡CH*), 2.37–2.51 (m, 2H, NCH_2*), 1.26–1.94 (m, 8H, 2CH_2 and 2CH_2*), 1.13 (d, $^3J_{HH}$ = 6.0 Hz, 3H, CH_3), 0.74 (d, $^3J_{HH}$ = 6.0 Hz, 3H, CH_3*); ^{13}C{^{1}H}-NMR δ_C (75.5 MHz; $CDCl_3$; Me_4Si) 139.1 (Ph), 137.5 (Ph), 133.8 (Ph), 133.6 (Ph), 128.6 (Ph), 128.1 (Ph), 128.0 (Ph), 127.9 (Ph), 127.5 (Ph), 127.3 (Ph), 81.9 (*C*≡CH), 79.3 (*C*≡CH*), 75.1 (C≡*C*H), 73.8 (C≡*C*H*), 56.3, 56.2, 54.7, 54.2, 51.8, 46.9, 33.2, 32.7, 22.2, 21.4, 20.8, 18.9. HRMS calcd for $C_{14}H_{17}N$: 199.1361. Found: 199.1358. MS (EI) *m*/*z*: 199 (2%), 184 (30), 115 (100), 89 (11). IR (neat oil) ν_{max}/cm^{-1} 3300m (C≡C–H), 3060w, 3030w, 2960s, 2871m, 2819m, 1492m, 1450m, 1376m, 1265m, 1136m, 1073w, 1030w, 947w, 741m, 698s, 642s.

The other compounds in Table 3 have been reported in the literature.[17c,40] The experimental details for these compounds can be found in the Supplementary Information, as well as ^{1}H and ^{13}C NMR spectra of all catalysis products in Table 3.

X-Ray crystallography

Crystals of appropriate dimension were obtained by slow diffusion of Et_2O into a solution of complex **8b** in CH_2Cl_2 at −18 °C. A crystal with approximate dimensions 0.21 × 0.19 × 0.17 mm^3 was mounted on a Mitgen cryoloop in a random orientation. Preliminary examination and data collection were performed using a Bruker Kappa Apex II Charge Coupled Device (CCD) Detector system single crystal X-Ray diffractometer equipped with an Oxford Cryostream LT device. All data were collected using graphite monochromated Mo Kα radiation (λ = 0.71073 Å) from a fine focus sealed tube X-Ray source. Preliminary unit cell constants were determined with a set of 36 narrow frame scans. Intensity data were collected using a combinations of ϖ and ϕ scan frames with typical scan width of 0.5° at a crystal to detector distance of 3.5 cm. The collected frames were integrated using an orientation matrix determined from the narrow frame scans. Apex II and SAINT software packages were used for data collection and data integration.[41] Analysis of the integrated data did not show any decay. Final cell constants were determined by global refinement of xyz centroids of 9055 reflections from the complete data set.

Collected data were corrected for systematic errors using SADABS based on the Laue symmetry using equivalent reflections.[41]

Crystal data and intensity data collection parameters are listed in Table S1.†

Structure solution and refinement were carried out using the SHELXTL-PLUS software package.[42] The structure was solved by direct methods and refined successfully in the space group *P*-1. Full matrix least-squares refinement was carried out by minimizing $\Sigma w(F_o^2 - F_c^2)_2$. The non-hydrogen atoms were refined anisotropically to convergence. All hydrogen atoms were treated using appropriate riding model (AFIX m3). A disordered molecule of Et_2O was located in the lattice as solvent of crystallization. The disorder was resolved with two orientations for all atoms with 50% occupancies and were refined with geometrical and displacement parameter restraints. Crystal data for **8b**: $C_{70}H_{56}Cl_2NO_2P_3Ru{\cdot}(C_4H_{10}O)$, M = 1282.16, T = 100(2) K, wavelength 0.71073 Å, triclinic, space group *P*-1, a = 13.6805(3) Å, b = 14.5594(3) Å, c = 17.2394(4) Å, α = 77.1170(10)°, β = 71.5080(10)°, γ = 71.6980(10)°, V = 3062.57(12) Å^3, Z = 2, density (calculated) = 1.390 Mg/m^3, absorption coefficient = 0.472 mm^{-1}, F(000) = 1328, theta range for data collection 1.49 to 26.39°, index ranges $-17 \leq h \leq 17$, $-18 \leq k \leq 18$, $-21 \leq l \leq 21$, reflections collected = 88 454, independent reflections, 12 305 [R(int) = 0.0428], completeness to theta = 25.00° (98.6%), absorption correction semi-empirical from equivalents, max. and min. transmission 0.9257 and 0.9077, refinement method full-matrix least-squares on F^2, data/restraints/parameters 12 305/176/806, goodness-of-fit on F^2 = 1.142, final R indices [$I > 2$sigma(I)] R_1 = 0.0459, wR_2 = 0.1271, R indices (all data) R_1 = 0.0632, wR_2 = 0.1489, largest diff. peak and hole 1.068 and −0.695 e.Å^{-3}.

Acknowledgements

We would like to thank the University of Missouri—Research Board for financial support. Funding from the National Science Foundation for the purchase of the NMR spectrometer (CHE-9974801), the purchase of the ApexII diffractometer (MRI, CHE-0420497) and the purchase of the mass spectrometer (CHE-9708640) are acknowledged.

References

1 Review and recent examples: (*a*) G. W. Kabalka and M.-L. Yao, *Curr. Org. Synth.*, 2008, **5**, 28; (*b*) O. Debleds, E. Gayon, E. Ostaszuk, E. Vrancken and J.-M. Campagne, *Chem.–Eur. J.*, 2010, **16**, 12207; (*c*) M. Kalek, T. Johansson, M. Jezowska and J. Stawinski, *Org. Lett.*, 2010, **12**, 4702; (*d*) V. Cadierno, J. Francos and J. Gimeno, *Organometallics*, 2011, **30**, 852; (*e*) N. P. Hiett, J. M. Lynam, C. E. Welby and A. C. Whitwood, *J. Organomet. Chem.*, 2011, **696**, 378.
2 R. Chinchilla and C. Nájera, *Chem. Rev.*, 2007, **107**, 874.
3 F. Amblard, J. H. Cho and R. F. Schinazi, *Chem. Rev.*, 2009, **109**, 4207.
4 A. Farwick and G. Helmchen, *Org. Lett.*, 2010, **12**, 1108.
5 (*a*) A. Hoepping, K. M. Johnson, C. George, J. Flippen-Anderson and A. P. Kozikowski, *J. Med. Chem.*, 2000, **43**, 2064; (*b*) N. Miyachi, F. Kanda and M. Shibasaki, *J. Org. Chem.*, 1989, **54**, 3511.
6 J. F. Lutz, *Angew. Chem., Int. Ed.*, 2007, **46**, 1018.
7 (*a*) N. Nomura, K. Tsurugi, N. Yoshida and M. Okada, *Curr. Org. Synth.*, 2005, **2**, 21; (*b*) T. Graening and H. G. Schmalz, *Angew. Chem., Int. Ed.*, 2003, **42**, 2580; (*c*) G. Helmchen, *J. Organomet. Chem.*, 1999, **576**, 203.
8 (*a*) R. J. Detz, H. Hiemstra and J. H. van Maarseveen, *Eur. J. Org. Chem.*, 2009, 6263; (*b*) N. Ljungdahl and N. Kann, *Angew. Chem., Int. Ed.*, 2009, **48**, 642; (*c*) Y. Miyake, S. Uemura and Y. Nishibayashi, *ChemCatChem*, 2009, **1**, 342.
9 A. G. Myers and B. Zheng, *J. Am. Chem. Soc.*, 1996, **118**, 4492.
10 V. Cadierno, P. Crochet, S. E. García-Garrido and J. Gimeno, *Dalton Trans.*, 2010, **39**, 4015.
11 L. Zani and C. Bolm, *Chem. Commun.*, 2006, 4263.
12 G. W. Kabalka and M.-L. Yao, *Curr. Org. Synth.*, 2008, **5**, 28.
13 V. Cadierno, J. Díez, S. E. García-Garrido, J. Gimeno and N. Nebra, *Adv. Synth. Catal.*, 2006, **348**, 2125.
14 Y. Nishibayashi and S. Uemura, *Curr. Org. Chem.*, 2006, **10**, 135.
15 G. Hattori, Y. Miyake and Y. Nishibayashi, *ChemCatChem*, 2010, **2**, 155.
16 Y. Imada, M. Yuasa, I. Nakamura and S.-I. Murahashi, *J. Org. Chem.*, 1994, **59**, 2282.
17 (*a*) G. Hattori, H. Matsuzawa, Y. Miyake and Y. Nishibayashi, *Angew. Chem., Int. Ed.*, 2008, **47**, 3781; (*b*) R. J. Detz, M. M. E. Delville, H. Hiemstra and J. H. van Maarseveen, *Angew. Chem., Int. Ed.*, 2008, **47**, 3777; (*c*) G. Hattori, K. Sakata, H. Matsuzawa, Y. Tanabe, Y. Miyake and Y. Nishibayashi, *J. Am. Chem. Soc.*, 2010, **132**, 10592; (*d*) A. Yoshida, G. Hattori, Y. Miyake and Y. Nishibayashi, *Org. Lett.*, 2011, **13**, 2460; (*e*) R. J. Detz, Z. Abiri, R. le Griel, H. Hiemstra and J. H. van Maarseveen, *Chem.–Eur. J.*, 2011, **17**, 5921.
18 (*a*) P. A. Evans and M. J. Lawler, *Angew. Chem., Int. Ed.*, 2006, **45**, 4970; (*b*) K. Kondo, Y. Kanda, A. Baba, K. Fukuda, A. Nakamura, K. Wada, Y. Morisaki and T. Mitsudo, *J. Am. Chem. Soc.*, 2002, **124**, 12960.
19 R. Sanz, D. Miguel, A. Martínez, J. M. Álvarez-Gutiérrez and F. Rodríguez, *Org. Lett.*, 2007, **9**, 727.
20 Z.-P. Zhan, W.-Z. Yang, R.-F. Yang, J.-L. Yu, J.-P. Li and H.-J. Liu, *Chem. Commun.*, 2006, 3352.
21 Y. Nishibayashi, M. D. Milton, Y. Inada, M. Yoshikawa, I. Wakiji, M. Hidai and S. Uemura, *Chem.–Eur. J.*, 2005, **11**, 1433.
22 (*a*) R. v. Ohri, A. T. Radosevich, K. J. Hrovat, C. Musich, D. Huang, T. R. Holman and F. D. Toste, *Org. Lett.*, 2005, **7**, 2501; (*b*) I. Matsuda, K. Komori and K. Itoh, *J. Am. Chem. Soc.*, 2002, **124**, 9072.
23 (*a*) S. Costin, N. P. Rath and E. B. Bauer, *Tetrahedron Lett.*, 2009, **50**, 5485; (*b*) S. Costin, N. P. Rath and E. B. Bauer, *Adv. Synth. Catal.*, 2008, **350**, 2414.
24 S. J. La Placa and J. A. Ibers, *Inorg. Chem.*, 1965, **4**, 778.
25 E. A. Shaffer, C. L. Chen, A. M. Beatty, E. J. Valente and H.-J. Schanz, *J. Organomet. Chem.*, 2007, **692**, 5221.
26 K. G. Caulton, *J. Am. Chem. Soc.*, 1974, **96**, 3005.
27 S. Gauthier, R. Scopelliti and K. Severin, *Organometallics*, 2005, **24**, 5792.
28 D. Amoroso, G. P. A. Yap and D. E. Fogg, *Organometallics*, 2002, **21**, 3335.
29 Reviews, recent applications and syntheses: (*a*) J. F. Teichert and B. L. Feringa, *Angew. Chem., Int. Ed.*, 2010, **49**, 2486; (*b*) I. S. Mikhel, H. Rüegger, P. Butti, F. Camponovo, D. Huber and A. Mezzetti, *Organometallics*, 2008, **27**, 2937; (*c*) L. A. Arnold, R. Imbos, A. Mandoli, A. H. M. de Vries, R. Naasz and B. L. Feringa, *Tetrahedron*, 2000, **56**, 2865.
30 S. Costin, N. P. Rath and E. B. Bauer, *Inorg. Chim. Acta*, 2008, **361**, 1935.
31 T. Leyssens, D. Peeters, A. G. Orpen and J. N. Harvey, *Organometallics*, 2007, **26**, 2637.
32 (*a*) H. A. Bent, *Chem. Rev.*, 1961, **61**, 275; (*b*) C. C. Levin, *J. Am. Chem. Soc.*, 1975, **97**, 5649.
33 C. A. Tolman, *Chem. Rev.*, 1977, **77**, 313.
34 T. J. J. Müller, *Eur. J. Org. Chem.*, 2001, 2021.
35 V. Cadierno and J. Gimeno, *Chem. Rev.*, 2009, **109**, 3512.
36 (*a*) M. Gruselle, C. Cordier, M. Salmain, H. El Amouri, J. Vaissermann and G. Jaouen, *Organometallics*, 1990, **9**, 2993; (*b*) K. M. Nicholas, M. Mulvaney and M. Bayer, *J. Am. Chem. Soc.*, 1980, **102**, 2508.
37 (*a*) A. Bartels, R. Mahrwald and K. Müller, *Adv. Synth. Catal.*, 2004, **346**, 483; (*b*) R. Riveiros, D. Rodríguez, J. Pérez Sestelo and L. A. Sarandeses, *Org. Lett.*, 2006, **8**, 1403; (*c*) N. Marion,

P. Carlqvist, R. Gealageas, P. de Frémont, F. Maseras and S. P. Nolan, *Chem.–Eur. J.*, 2007, **13**, 6437.
38 Varying amounts of Et_2O were always observed in the ^1H NMR spectra of **8**, even after elongated periods of drying, and the X-Ray structure of **8b** also contains an ether molecule in the crystal lattice. Ruthenium-coordinated ether can also be observed in the ^1H NMR of the complexes **8**, giving broad shifts around 5.8 and 2.2 ppm.
39 Due to the numerous aromatic carbon atoms, a complex aromatic region in the ^{13}C NMR spectra resulted. These generally uninformative signals were not listed.
40 (*a*) G. Quash, G. Fournet, C. Courvoisier, R. M. Martinez, J. Chantepie, M. J. Paret, J. Pharaboz, M. O. Joly-Pharaboz, J. Goré, J. André and U. Reichert, *Eur. J. Med. Chem.*, 2008, **43**, 906; (*b*) T. Sugiishi, A. Kimura and H. Nakamura, *J. Am. Chem. Soc.*, 2010, **132**, 5332; (*c*) H. Frey and G. Kaupp, *Synthesis*, 1990, **10**, 931; (*d*) J. R. Brooks, D. N. Harcourt and Roger D. Waigh, *J. Chem. Soc., Perkin Trans. 1*, 1973, 2588.
41 Bruker Analytical X-ray, Madison, WI, 2010.
42 G. M. Sheldrick, *Acta Crystallogr., Sect. A: Found. Crystallogr.*, 2007, **64**, 112.

